The application of the X-ray micro-diffraction to study some industrial problems

H. J. Krztoń,[a)] M. Niesler, Z. Kania
Instytut Metalurgii Żelaza, Gliwice, Poland

[a)] Electronic mail: hkrzton@imz.pl

The X-ray micro-diffraction laboratory technique was applied to study the quantitative changes of austenite content in TRIP steels after deformation and to reveal the phase composition of precipitates in an inner part of a hearth of a blast furnace. The usefulness of this technique was shown by calculating the austenite content after tensile test in three different parts of a small tensile test sample and after a clinching test in two areas of a clinching joint. The calculations showed the decrease in austenite content in deformed parts in comparison to not deformed areas. The presence of various kinds of chlorides, including the iron oxide chloride hydroxide in a sample taken from a graphite refractory lining of blast furnace, was confirmed by micro-diffraction patterns.

Key words: X-ray micro-diffraction, austenite, TRIP steels, clinching joint, alkali chlorides, iron blast furnace

I. INTRODUCTION

Some new fields of application of X-ray diffraction can be introduced owing to new or up-graded components of the modern X-ray laboratory diffraction systems. A good example is a micro-diffraction technique with a mono-capillary as a primary beam optical part (Fransen *et al.,* 2001) in connection with a relatively strong X-ray laboratory source and a high-efficient, fast detector. This technique gives the unique opportunity to study a microstructure transformation during plastic deformation in TRIP (Transformation-Induced Plasticity) steels, using small tensile specimens. The microstructure of TRIP steels consists of ferrite, bainite and up to 15 mass% of metastable retained austenite which is progressively transformed to martensite during deformation (Traint *et al*., 2006; Grajcar and Krztoń, 2009) and this transformation is related to an additional absorption of energy during crash events and increases the level of safety. There is also a requirement of research the changes in local austenite content in a clinching process as a new technique replacing the spot welding process (Mucha et *al.*, 2011).

https://doi.org/10.1017/S0885715613001085 Published online by Cambridge University Press

In steel industry, the formation and presence of various chemical compounds in a blast furnace have got an important influence on working conditions, stability and a mean life of a blast furnace. One of the most important problems is the role of chlorine and its interaction with other elements, present in the atmosphere of a blast furnace (Lectard *et al.*, 2004). There are three typical sources of chlorine i.e. blast furnace burden, coke and injection coal and also some new input materials, concerned with the recycling of waste materials (as plastics) (Niesler and Stecko, 2000). The micro-diffraction technique can be capable of studying the formation and identifying the crystalline compounds precipitated during the working time of a blast furnace.

II. EXPERIMENTAL

The chemical compositions of steel samples are shown in Table I. The chemical compositions were obtained by means of a Bruker Magellan Q8 optical emission spectrometer with spark excitation. The surfaces of the steel samples were prepared for X-ray diffraction experiments by cutting, polishing and finally etching to eliminate the influence of mechanical treatments on stability of austenite. Then they were placed on a micro-diffraction stage, with z-(vertical) axis adjustment and controlled X-Y movements. Figure 1 shows a cross-section of a tensile test piece after a tensile test. The second steel sample (see the cross-section of the sample in Figure 2) was formed as a clinching joint of two pieces of steel sheets of chemical composition given in Table I.

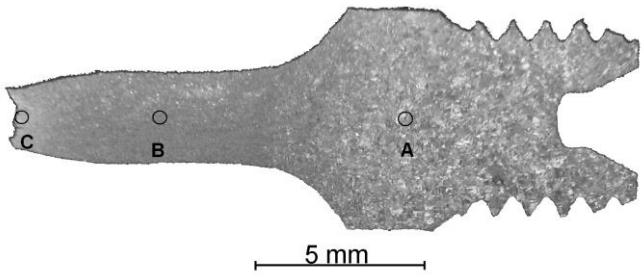


Figure 1. The cross section of a tensile piece after the tensile test. One of the experimental arrangements of the investigated areas is marked by the circles A, B and C. A = the area in the original, not deformed material, B = the area in the deformed part, C = the area close to the point of tensile failure.

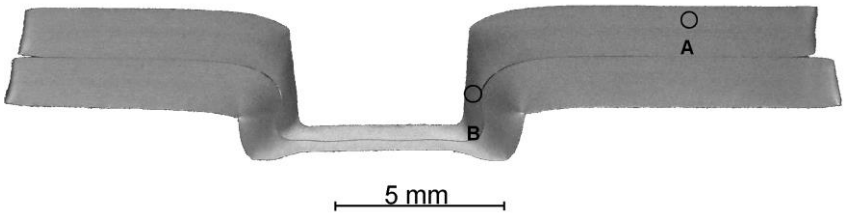


Figure 2. The cross section of a clinching joint of two pieces of steel sheets. The investigated areas are marked by the circles A and B. A = the area in the original, not deformed material, B = the area in the deformed part.

https://doi.org/10.1017/S0885715613001085 Published online by Cambridge University Press

Table I. Chemical composition of the steel samples (wt.%). The balance is Fe.

Sample	C	Si	Mn	Al	S	P	Cu	Ti	Nb	Sn
Tensile Piece	0.20	0.20	1.50	1.50	0.012	0.015	0.21	-	-	0.008
Clinching joint	0.162	0.54	1.92	0.78	0.000	0.007	0.022	0.002	0.002	-

The next two examples of examination of the very local phase composition are concerned with the inclusions in a graphite refractory lining of an iron blast furnace. The pieces of the graphite refractory lining were taken from an inner part of a hearth of a blast furnace by drilling. The pieces were examined using light microscopy to find the location of precipitates and then were cut into smaller samples which could be situated on the micro-diffraction stage. Before the data collection, the examined surfaces of all specimens were controlled by a special device, indicating the z position, and by a camera showing the surface of the piece towards a goniometer axis and a position of the centre of the beam. The X-ray diffraction data were collected at room temperature (23 ^{o}C) on a PANalytical Empyrean $\theta - \theta$ diffractometer (50 kV, 45 mA) equipped with a micro-diffraction attachment, a cobalt X-ray tube (λ=0.17903 nm) with a point focus and a PIXcel detector in 1D mode. An iron filter, placed between the X-ray tube and a specimen, was used to eliminate the Co $K\beta$ radiation. A collimator with a monocapillary of an inner diameter of 0.3 mm was mounted on the primary beam. The size of the diameter of the beam on the samples was approximately 0.4 mm. The steel specimens were measured within a 2θ angular range of 46^{o}-104^{o}, with a step size of 0.02626^{o} 2θ and step counting time of 600 s. The three independent experiments were performed on each part of the samples; the location of the surface was arranged each time irrespective of the previous position. The calculations of the austenite content in tensile test specimen were done using the Averbach-Cohen method (Jatczak *et al.,* 1980). The integral intensity of each reflection was determined using the HighScore Plus software package (PANalytical, The Netherlands, V. 3.0). The austenite fractions in the next specimen which was a clinching joint were found as the results of the Rietveld refinement (Rietveld, 1969) using the Siroquant V.3 program (Taylor, 1991). The instrumental zero point and background shape were refined for the whole diffraction patterns. The scales, the unit cell dimensions, the halfwidth parameters were refined for both kinds of phases (α phase with space group $Im\bar{3}m$ and

https://doi.org/10.1017/S0885715613001085 Published online by Cambridge University Press

γ phase with space group $Fm\bar{3}m$). A Pearson VII function was chosen to calculate the shape of diffraction lines.

The measurements of a specimen taken from a graphite refractory lining were carried out within a 2θ angular range of 10^{o}- 90^{o}, with a step size of 0.01313^{o} 2θ and step counting time of 900 s. The chemical analysis of the investigated precipitates in a graphite refractory lining of an iron blast furnace was determined by scanning electron microscope Philips XL 30 with SE (secondary electrons), BSE (backscattered electrons) and EDS (Energy-dispersive X-ray spectroscopy) detectors.

III. RESULTS AND DISCUSSION

The SEM micrographs of the measured areas of the tensile test specimen and the corresponding diffraction patterns are shown in Figure 3. The changes of the microstructure, depending on the place of the sample can be observed - from ferritic-bainitic structure in the not deformed area [Figure 3(a)], containing 7.5vol. % of austenite [Figure 3(f)], through the clearly seen the ferrite-bainite-martensite microstructure with 4.9vol.% of austenite [Figures 3(b) and 3(e)], to the strongly deformed area near the point of tensile failure [Figures 3(c) and 3(d)] with 2.1vol.% of austenite (Table II). The smallest austenite content is close to the detectability limit in such experiments and difficult to determine, hence the largest value of error can be expected. The diffraction pattern of the not deformed part of the sample consists of two kinds of the reflections; three of them belong to austenite phase and three to ferrite phase (α phase) which can be found in two distinct states: as a component of bainitic phase and as an individual component of the microstructure. After a tensile test, in the deformed part of the specimen, the formation of martensite phase was observed [Figures 3(b) and 3(c)]. First, the Rietveld refinement was introduced to calculate the fractions of austenite (Figure 5), assuming the presence of one α phase. In Figure 5, two overlapped but distinguishable reflections appear in the range of the position of (200) reflection of α phase. Such a difference does not correspond to the totally overlapped reflections of (110) type and the contributions of phases of α-type to the observed reflection of (110) type cannot be separated. Moreover, the broadening of the reflections does not fit the usually applied in Rietveld refinements formula of angular dependence of peak width (Prince, 1993).

https://doi.org/10.1017/S0885715613001085 Published online by Cambridge University Press

Table II. The quantitative results, obtained as volume fractions of austenite in three different areas of tensile piece (as shown in Figure 1). The results are the mean values, calculated from three experiments (see the text).

Area	Vol.%
A	7.5 ± 0.9
B	4,9 ± 0,7
C	2.1 ± 1.5

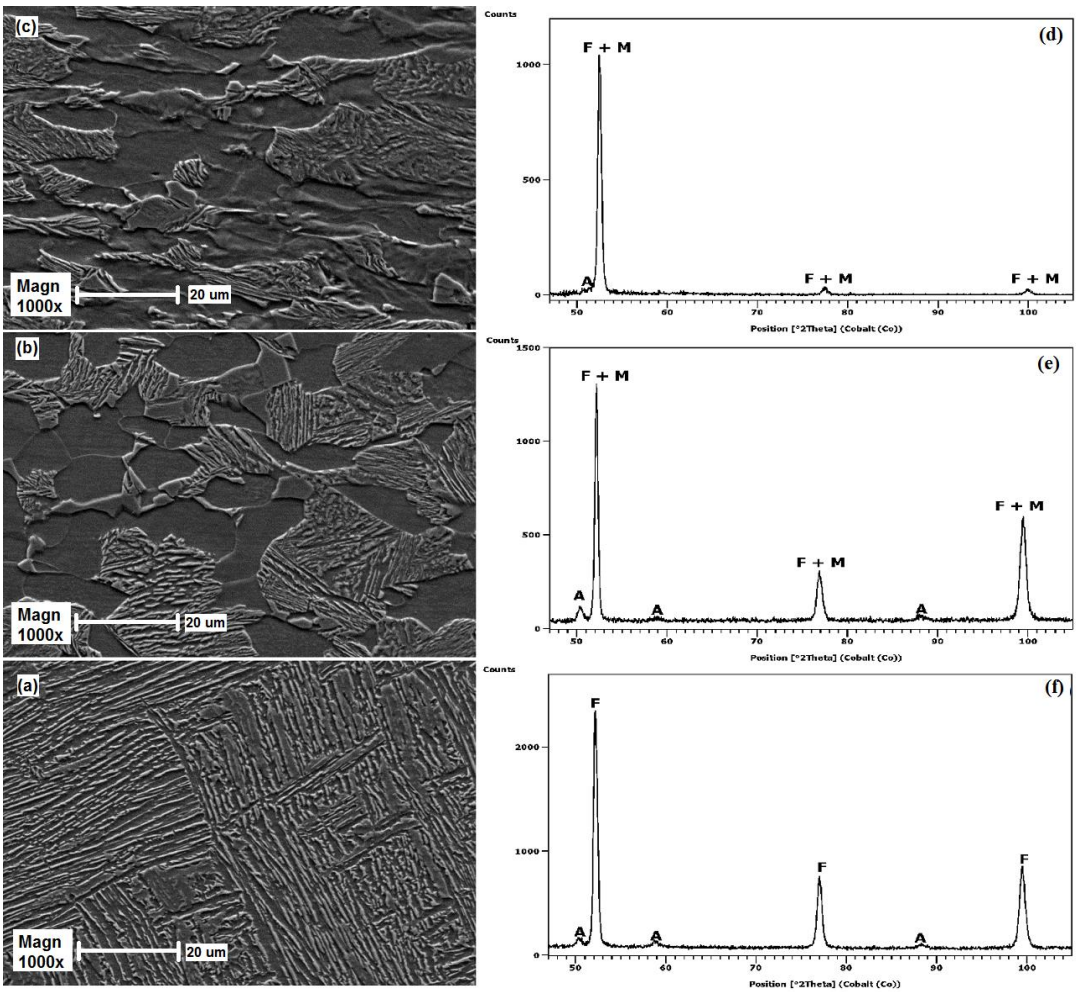


Figure 3. The microstructures of three areas of the tensile test sample (SEM images with a SE detector) and the corresponding X-ray micro-diffraction patterns. (a): the area in the original, not deformed material; (b): the area in the deformed part; (c): the area close to the point of tensile failure; (d) – (f): the diffraction patterns of the (c) – (a) areas, respectively.
SEM = scanning electron microscopy, SE = secondary electrons
A = austenite, F = ferrite, M - martensite

https://doi.org/10.1017/S0885715613001085 Published online by Cambridge University Press

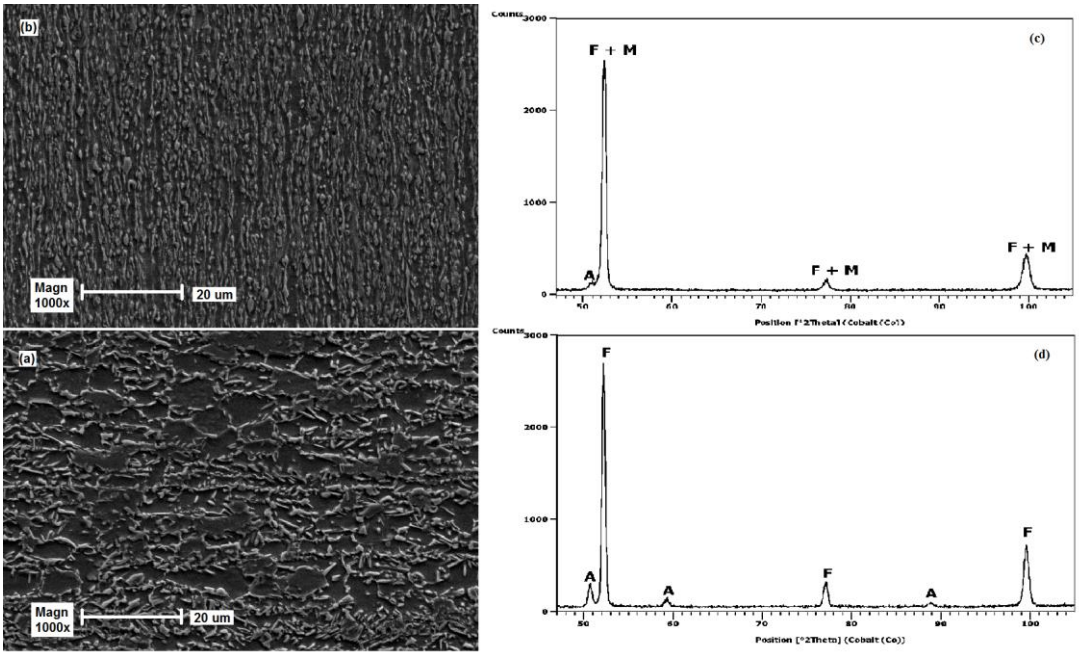


Figure 4. SEM micrographs (SE detector) of two chosen areas of a clinching joint [(a), (b)] and the corresponding X-ray micro-diffraction patterns [(d), (c)].
SEM = scanning electron microscopy, SE =secondary electrons

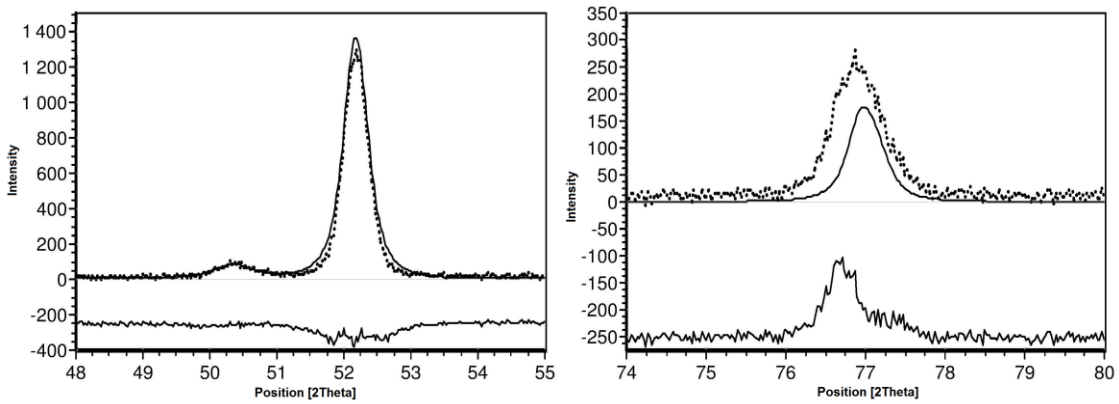


Figure 5. Observed (dots), calculated (solid line) and difference Rietveld plots of two chosen ranges of 2θ, corresponding to the positions of (111) reflection of austenite and (110) reflection of ferrite/martensite (left) and the position of (200) reflection of ferrite/martensite. Tensile sample, the B area in the deformed part. Goodness-of-fit $\chi = 1.90$ ($\chi = R_{wp}/R_{exp}$), R-F=0.503.

Hence, the integral intensity of each peak was determined separately and the Averbach-Cohen method was applied to calculate the austenite fractions.

Figure 4 reveals the microstructures (SEM micrographs, SE detector) of two areas of the clinching joint [Figure 4(a) – not deformed part A, Figure 4(b) – the deformed area B] and their diffraction patterns as seen in Figures 4(d) and 4(c), respectively. The microstructure is much finer than the tensile specimen's microstructure. Furthermore, the application of the Rietveld method was possible to determine the austenite contents in both examined areas (Table III, IV). As an

https://doi.org/10.1017/S0885715613001085 Published online by Cambridge University Press

example, the result of the Rietveld refinement for not deformed area is shown in Figure 6. The model of one α phase was introduced in Rietveld refinement, assuming that both ferrites (ferrite as an individual phase and 'bainitic' ferrite) having the same unit cells.

Table III. The quantitative results, obtained as weight fractions of austenite in two different areas of clinching joint (as shown in Figure 3). The results were obtained from the Rietveld refinement, assuming the presence of one α phase in the calculations. α phase (ferrite/ martensite) – space group $Im\bar{3}m$; γ phase (austenite) – space group $Fm\bar{3}m$.

Area	Wt.%
A	12.5 ± 0.6
B	4,4 ± 0,4

Table IV. Clinching joint. The values of errors, calculated by Siroquant (Siroquant V.3, Technical and Clay Manuals, 2006). The calculated errors are the square roots of the diagonal elements of the least-squares variance-covariance matrix, and are the "estimated standard deviations", of the weight percentages. Actual values of errors are given using goodness-of-fit χ (Prince,1993).

Phase	Wt.%	Calculated Error, e	χ	Actual Error e* χ
Austenite in the A area	12.5	0.45	1.30	0.59
Austenite in the B area	4,4	0.25	1.31	0.33

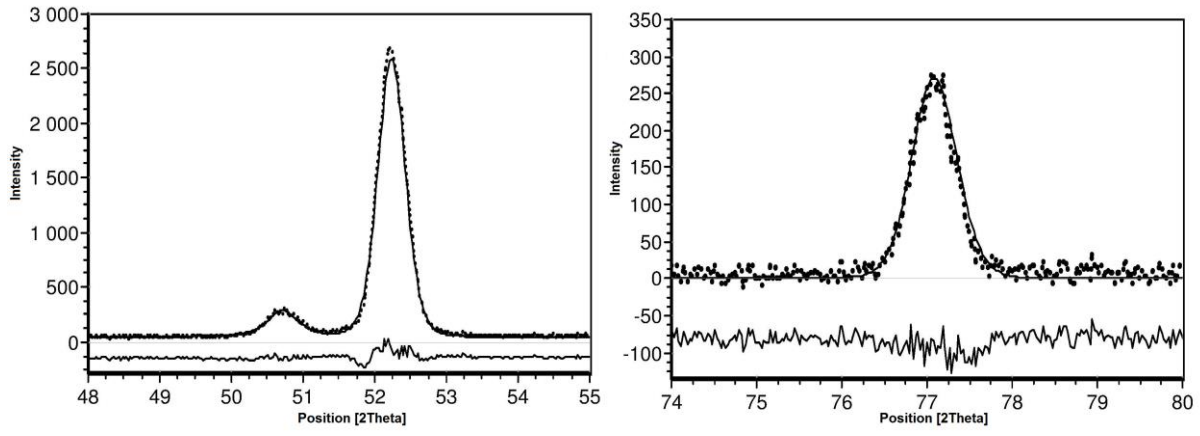


Figure 6. Observed (dots), calculated (solid line) and difference Rietveld plots of two chosen ranges of 2θ, corresponding to the positions of (111) reflection of austenite and (110) reflection of ferrite (left) and the position of (200) reflection of ferrite. Clinching joint, the A area in the original, not deformed material. Goodness-of-fit χ = 1.30 ($\chi = R_{wp}/R_{exp}$), *R-F*=0.115.

https://doi.org/10.1017/S0885715613001085 Published online by Cambridge University Press

To study the formation of compounds containing chlorine in an industrial blast furnace, a piece from a sample taken from a graphite refractory lining was positioned on the micro-diffraction sample holder and two areas were chosen to investigate [Figures 7(a) and 7(b)]. A camera, showing the surface of the piece towards a goniometer axis and a position of the centre of the beam (a cross in the picture), was used to make a photograph of the surface. The diffraction patterns confirmed the presence of potassium chloride [Figure 7(c)] and sodium chloride [Figure 7(d)]. The SEM micrograph and the corresponding X-ray energy dispersive spectrum of the analyzed inclusion of KCl are shown in Figure 8. A complex chloride, containing both potassium and sodium, was also found. Moreover, the chlorine interacts with iron, forming iron oxide chloride hydroxide – akaganeite [Figure 7(d)].

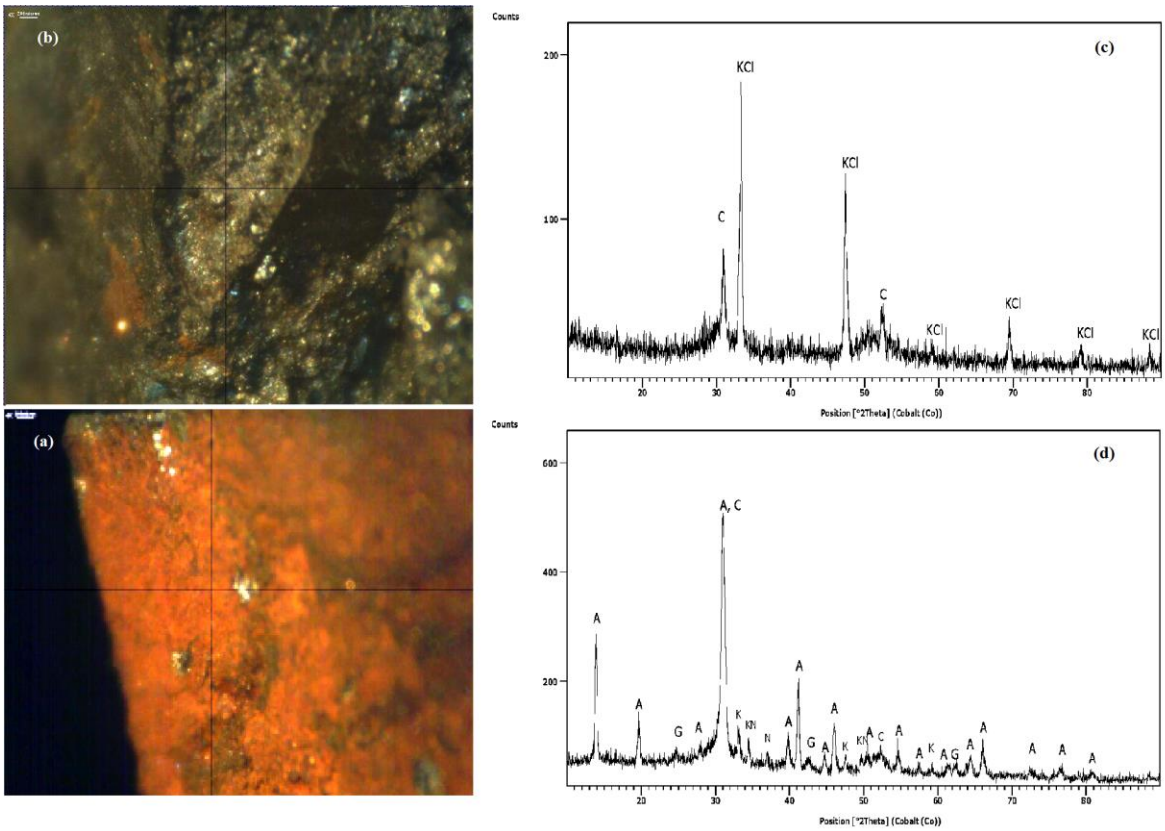


Figure 7. The two analyzed surfaces of a sample of the graphite refractory lining, taken from an inner part of a hearth of a blast furnace and the corresponding X-ray micro-diffraction patterns. K = sylvite KCl, KN = sodian sylvite $K_{0.6}Na_{0.4}Cl$, N = halite NaCl, C = graphite, G = goethite α-FeO(OH), A = akaganeite-M $Fe_8(O,OH)_{16}Cl_{1.3}$

https://doi.org/10.1017/S0885715613001085 Published online by Cambridge University Press

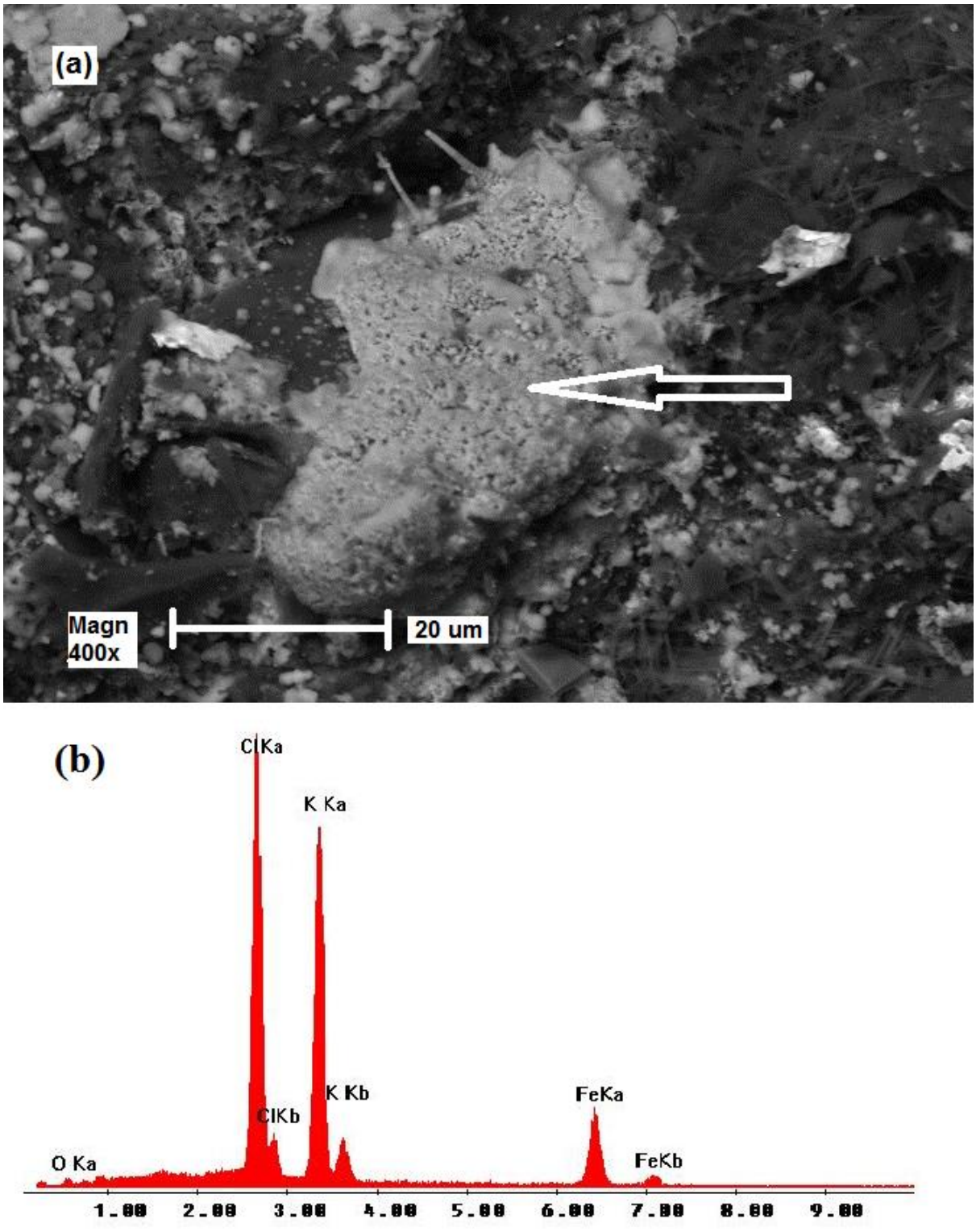


Figure 8. SEM micrograph [BSE detector – (a)] and the corresponding EDS result of a point chemical analysis (b). An arrow indicates the point of analysis. The detection of Fe and O is concerned with the presence of iron oxide hydroxide in the vicinity of the KCl particle.

SEM = scanning electron microscopy, BSE = backscattered electrons,
EDS = Energy-dispersive X-ray spectroscopy

https://doi.org/10.1017/S0885715613001085 Published online by Cambridge University Press

IV. CONCLUSION

The laboratory X-ray micro-diffraction technique can be successfully applied to determine both qualitative and quantitative local phase compositions. The main advantage of this application is the possibility to follow the quantitative changes in austenite content in different parts of the test samples made of TRIP steels after various kinds of deformation. Hence, this is a capability to carry out some model investigations on a small scale. The study of a graphite refractory lining of an industrial iron blast furnace confirmed the existence of crystalline chlorine compounds, as KCl, NaCl and $K_{0.6}Na_{0.4}Cl$. The unexpected build-in of chlorine atoms in iron oxide hydroxide was observed.

ACKNOWLEDGMENTS

The authors would like to thank Professor Roman Kuziak and M. Adamczyk, MSc from Institute for Ferrous Metallurgy for providing the steel samples.

Fransen, M. J., Vasterink, J. H. A. and te Nijenhuis, J. (**2001**). "Micro-diffraction with mono-capillaries," Adv. X-ray Anal. **44**, 284-289.

Grajcar, A. and Krztoń, H. (**2009**)."Effect of isothermal bainitic transformation temperature on retained austenite fraction in C-Mn-Si-Al-Nb-Ti TRIP type steel," J. Achieve. Mater. Manuf. Eng. **35**, 169-176.

Jatczak, Ch. F., Larson, J. A., and Shin, S. W. (**1980**). "Retained austenite and its measurements by X-ray diffraction," SAE Technical Paper 800426 [SP-453], Society of Automotive Engineers, Inc [doi:10.4271/800426.].

Lectard, E., Hess, E. and Lin, R. (**2004**). "Behavior of chlorine and alkalis in the blast furnace and effect on sinter properties during reduction," Rev. Metall. (Les Ulis, Fr.) **101**, 31-38.

Mucha, J., Kaščak, L. and Spišák, E. (**2011**). "Joining the car-body sheets using clinching process With various thickness and mechanical property arrangements," Arch. Civil Mech. Eng. **11**, 135-148.

Niesler, M. and Stecko, J. (**2000**). "Ocena możliwości utylizacji odpadów tworzyw szt ucznych w wielkich piecach," Hutnik – Wiadomości Hutnicze **67**, 78-85.

Prince, E. (**1993**). "Mathematical aspects of Rietveld refinement" in *The Rietveld method*, edited by R. A. Young, (Oxford University Press, New York), 43-54.

Rietveld, H. M. (**1969**). "A profile refinement method for nuclear and magnetic structures,"

https://doi.org/10.1017/S0885715613001085 Published online by Cambridge University Press

J. Appl. Crystallogr. **2**, 65-71.

Sietronics Pty Limited. (**2006**). Siroquant V.3 Technical and Clay Manuals (Computer Software), Sietronics Pty Limited.

Taylor, J. C. (**1991**). "Computer programs for standardless quantitative analysis of minerals using the full powder diffraction profile," Powder Diffr. **6**, 2-9.

Traint, S., Pichler, A., Sierlinger, R., Pauli, H. and Werner, E. A. (**2006**). "Low-alloyed TRIP-steels with Optimized Strength, Forming and Welding Properties," Steel Res. Int. **77**, 641-649.

https://doi.org/10.1017/S0885715613001085 Published online by Cambridge University Press